AADE-17-NTCE-104

Use Of Advanced Gas Migration Model To Optimize Zonal Isolation

Axel-Pierre Bois, Manh-Huyen Vu, Greg Galdiolo, Anthony Badalamenti, CURISTEC

Abstract

One of the main objectives of primary cementing is to prevent the percolation of gas through a cemented annulus, which can result in channels in the cement sheath. Gas channeling, once established, has proven to be extremely difficult and costly to repair.

The most current theory used to explain gas migration is the early gelation of the cement slurry, which leads to a decrease of hydrostatic pressure within the cement annulus. Over the years, various models have been developed, most of them revolve around the concepts of static gel strength (SGS), critical static gel strength, (CSGS), and transition time.

Unfortunately, these approaches have failed to accurately predict gas migration. One of the main reasons for this failure is that these approaches are based on fluid-mechanics theories, and do not take into account the cement phase changes during hydration (fluid to solid). Additionally, most models do not take into account the true mechanisms at the origin of gas percolation: Matrix, chimney, and micro-annulus.

This paper presents a new gas migration model that eliminates these drawbacks. It considers two different stages in the life of the cement sheath (fluid-type and porous-solid type), and is characterized by constitutive laws, which are integrated over the length of the cement column by time to determine if gas migration will occur and what are the mechanisms according to which it will occur.

Introduction

Gas migration is defined as gas entry into a cemented annulus with the potential to provide a flow path for formation fluids, including gas, water and hydrocarbons, into the wellbore. This can result in fluid flow in the annulus and into another reservoir or to the surface. The severity of the problem[1] ranges from the most hazardous (e.g., a blowout situation arising from a severe pressure imbalance) to the most marginal (e.g., a residual gas pressure of a few psi at the wellhead). Detecting annular fluid flow is very difficult, sometimes it can be done using cement bond logs or by noticing unexpected pressures at the wellhead or surface casing-vents (SCV). Inter-zonal flow (from one reservoir to another) is more difficult to detect due to the well architecture and current analytical methods.

The cementing industry first recognized gas migration in the early 1960s[2], and since then, the industry has dedicated millions of research dollars to understanding the mechanics of gas migrations and developing solutions. Today there is a vast quantity of literature that describes various aspects of gas migration:

- Field-case study analyses and experiments for making practical recommendations[2,3,4,5,6].
- Laboratory investigations to improve the understanding of gas migration fundamentals [7,8,9,10,11,12].
- Development of technical solutions[13,14,15,16,17,18,19].
- Applications of new products and techniques in the field[20,21].
- Empirical qualitative prediction techniques[22,23].

However, successful numerical simulations of the process or scaled laboratory experiments that could allow a generalized and quantitative prediction of gas migration have not been reported[1] and gas migration problems still occur[24], showing that the problem is not solved yet. The main reason for this fact seems to be that gas migration is a multi-process mechanism, while most proposed solutions look at single processes.

Therefore, this paper aims at presenting a holistic, multi-process mechanism model of gas migration that is able to perform quantitative predictions.

Conditions that favor gas migration

Numerous authors[1,24,25,26] have published state-of-the-art gas migration papers. One of them[1] identified that there are three distinct conditions that must occur at the same time for annular gas migration to take place:

- The hydrostatic pressure in the annulus must fall to a level that is less than or equal to the pore pressure of a gas-bearing zone.
- There has to be a space in the annulus that allows gas entry.
- A path must be present in the annulus through which the gas can migrate.

Two of these conditions require some comments:

- The underbalanced condition uses the expression “pressure in the annulus” without clarifying which pressures it is. One can distinguish at least two stages: When the cement slurry is a liquid, the pressure is the fluids hydrostatic pressure; When the cement slurry has become a weak porous material, the pressure can be the pore pressure within the porous material or the total stress, depending on the case.

- The "space in the annulus" condition does not represent a true mandatory condition as, most of the times, the pathways are filled with a fluid and there is no available space stricto sensu. What we have is a compressible gas and a pathway filled with a fluid that is mobile enough to permit its displacement.

Hence, only two conditions are analyzed in the following sections of the paper, i.e., the mechanisms that put cement in an underbalanced condition and the pathways for gas migration. Preventing gas migration can be accomplished by ensuring that the two conditions never occur at the same time.

Furthermore, Stiles[1] proposes to divide cement life into three stages: 1) During placement (immediate); 2) Post-placement (short term); and 3) Post setting (long term). However, as cement hydration progresses, its physical state changes from a liquid slurry (during placement), to a high permeability, weak porous solid (when setting), and, finally, to a low-permeability porous solid (after hardening). Therefore, cement-sheath life should be divided into six stages (Figure 1), with only stage 2 to 5 being concerned by gas migration.

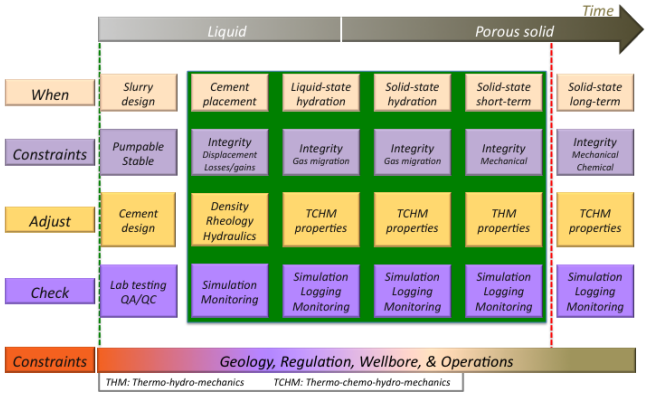

Figure 1. The six periods of the life of a cement sheath

Underbalanced condition

Cooke et al.[4] observed that there are two mechanisms which must occur at the same time for pressure in the annulus to decrease: The first one should lead to a decrease in cement volume and the other one should prevent cement axial displacement. Indeed, if a decrease in cement volume occurs without a restriction to the cement sheath axial displacements, this should not lead to a decrease in pressure.

Overall, the main factors that can lead for pressure in the annulus to be less than or equal to the pore pressure of a gas-bearing zone are:

- Cement placement: Low fluid densities can lead to dynamic (during placement) or static (just after the bump of the plug) pressures which can be less than or equal to the pore pressure of the gas-bearing zone.
- Liquid-state hydration[7,8,9,10,14,27,28,29,30,31]: Gel strength development can prevent slurry axial displacements and fluid loss can result in annular bridging, an increase in slurry-gelation (caused by a reduced water content in the slurry), and a decrease in the height of the column (owing to a slurry-volume decrease).
- Solid-state hydration[13]: Cement hydration mechanics can cause cement shrinkage, which results in a decrease in slurry volume.
- Liquid-state and solid-state hydration[7,14,29]: Heterogeneous cement gelling or hydrating can prevent slurry axial displacements. This can result from 1) Cement batch heterogeneity; 2) Non-uniform geothermal temperature in transient state; 3) Localized drained hydration in front of an aquifer, while the rest of the cement is hydrated under undrained conditions, because drained hydration leads to an increase in volume and then to a restriction in cement axial displacement; 4) Localized large fluid loss, because this can be associated to a thick mud/cement cake that would restrict slurry axial displacement; and 5) Change in thickness of the cement sheath along the well (due to wellbore cavings, mud/cement cake, tubular OD, tool joints…) as thicker cement sheath means faster hydration because of the thermo-activated nature of cement hydration.

Leakage pathways

Gas migration does not only need an underbalanced pressure condition, but also requires a leakage pathway across barriers for fluid to migrate from one reservoir to another. Based on the wellbore geometry, four types of pathways can occur: 1) Channels formed in the cement sheath; 2) The interface between the cement sheath and the casing; 3) The interface between the cement sheath and the formation; and 4) Channels formed in a damaged formation.

The main factors that can lead to the creation of cement pathways (channels) are[15,29]:

- Cement placement[7,32]: Drilling mud channels can act as fluid flow paths. They are typically the result of either or a combination of low casing standoff and poor well fluid displacement mechanics. As the drilling mud in these channels dehydrates the drilling mud either shrinks or cracks resulting in an increase in permeability therefore facilitating fluid migration.
- Liquid-state hydration[15,17,33,34,35,36]: Cementing systems that exhibit high fluid loss may create areas within the cement matrix that gas can occupy. As the gas in these areas expands during cement transition the gas bubble buoyancy will change and begin coalescence, thereby creating gas channels (chimneys) in the annular cement column.
- Solid-state short-term[37,38]: Changes in wellhead pressure and in wellbore fluid densities and temperatures can damage cement after it has set. Typically the cement damage modes will be either micro-annuli or cracks, which can create fluid flow pathways.

The main mechanisms that can create voids at the interface between the cement sheath and the casing are:

- Cement placement: If the casing is not properly cleaned prior to cementing there is a risk that the ce-

ment/casing hydraulic bond will be low, thereby resulting in a micro-annuli. This will create a fluid flow path.

- Solid-state hydration and short-term[37,38]: If a micro-annulus is formed due to cement hydration or a decrease in wellbore temperature or pressure, it could serve as a pathway for gas migration if gas can migrate to the inner boundary of the cement sheath.

The main mechanisms that can create voids at the interface between the cement sheath and the formation are:

- During drilling: Drill cutting beds caused by poor wellbore cleaning techniques can create fluid flow paths. Additionally drilling mud high fluid loss builds mud cakes that can remain non-displaced by the cement slurry and later suffer from drying or cracking, hence creating permeable pathways. However, if these pathways would occur in front of reservoirs and not in front of barriers, their effect should be negligible in terms of leakage paths.
- Liquid-cement hydration: Cement fluids loss and free fluid can be major contributors to gas migration if not addressed in the cement design. Cementing a highly deviated or horizontal well with a slurry designed with a high free fluid content was studied by various authors, giving contradictory results. Tinsley et al.[14] concluded that, although undesirable, free water would not be an influential factor with respect to annular gas flow. Conversely, Webster and Eikerts[9] observed that, in deviated holes, the free water could coalesce to form a continuous channel on the upper side of the hole, forming a path through which the gas may migrate. They recommended that a cement slurry be designed with essentially no free water. Shipley and Mitchell[39] observed that the cement transition time is reduced with the angle of inclination and that the hydrostatic pressure will decrease more rapidly. As a result, there would exist a free fluid threshold that is related to the inclination angle at which the stabilized gas rate reaches its maximum value. Additionally fluid loss builds cement cakes with the same consequences as mud cakes.
- Solid-state hydrating[37,38]: If a micro-annulus is created during cement hydration or due to a decrease in temperature, for example, it could serve as a pathway for gas migration. However, it should be noted that the creation of such a micro-annulus requires that the hole remains stable after its creation; otherwise it is not a micro-annulus that will be created but a damaged zone. Furthermore formation creep could close the micro-annulus over time.

Pathways through formation are created during drilling, cement hydration, or cement early age:

- During drilling: When drilling overbalanced, the mud density should be high enough for the drilling mud pressure to be greater than the formation pore pressure and for the formation not to fail, creating an enlarged wellbore due to breakouts. Formation breakout can have two types of consequences for fluid migration after cementing: 1) The creation of formation damage zones with larger permeability where fluid could migrate in the future; and 2) The creation of a wellbore with excessive washouts which decreases drilling mud displacement and casing centralization, therefore increasing the probability of drilling mud channels in the annular cement column. Conversely, the drilling mud density should not be greater than the formation's fracturing pressure. Otherwise fractures could be induced at the wellbore wall, which may serve as leakage paths for fluid migration after cementing.
- Cement placement: Cement placement is a dynamic process whereby cement slurries displace the mud in the annulus between the casing and the wellbore. Therefore, fluid pressure in the annulus is a function of numerous variables such as the rheology and density of the various fluids, the compatibility of the fluids, the trajectory of the well, the diameters of wellbore and casing, the casing standoff, wellbore washouts or restrictions due to hole collapse, the formation temperature, and the conditions under which the fluids are pumped (pressure, temperature). In the same manner as it was required during drilling, wellbore pressure should be greater than the formation pore pressure and large enough for the formation not to fail. It should also not be too large because this could induce tensile fractures in the formation.
- Liquid-state and solid-state hydration: Cement fluid loss and cement hydration can lead to a decrease in the pressure/radial stress within the cement, which may lead to damaging the cement sheath, thereby creating a fluid leak path;
- Solid-state early age[40]: The geochemical interaction between cement and shale may alter shale behavior, hence leading to a local damaged zone at the interface. This damaged zone could serve as a pathway for gas migration.

Suitability of lab testing for gas migration

Over the years, the industry has developed many gas migration laboratory test devices. Most of them have limitations that can affect their ability to be realistic to actual well condition. Many times, it is not clear if the gas migration experiment results are related to matrix flow or to in-flow through a micro-annulus at the inner boundary of the cell. If the test results are due to cement matrix flow, it would mean that the measurements are close to a cement intrinsic characterization, however if the gas flow measurement are due to micro-annulus flow, the measurements should be viewed as test cell-design dependent, indicating that the tests would not characterize the cement slurry resistance to gas migration. For example, Stewart and Schouten[17] conducted gas migration tests that showed that the combined effects of heating (expansion) and cement shrinkage (contraction) could create a micro-annulus at the cement/steel interface, meaning that the meas-

urements could become useless if their objective is to evaluate if the cement slurry can prevent gas flow through its matrix. These tests were later confirmed by Martins et al.[41]. On the opposite, Degouy and Large[42] developed a test cell where gas injection and detection systems were immersed in the cement slurry. However, due to the length of the test cell (43 cm), the gas injection and detection systems were spaced very close together which gave very pessimistic results.

Today, most gas migration test cells are limited in length, therefore the potential for gas migration is measured over a very short interval that is not representative of what actually occurs in the well. Additionally, most cells mimic a cement plug and not a cemented annulus, which is not an issue when measuring the cement's intrinsic behavior. However this is not the case because the measurements are sensitive to the test cell's length, diameter, stiffness and operating conditions. As a consequence, most test cells do not allow for testing the cement-annulus interface or for characterizing the cement intrinsic behavior.

Suitability of numerical modeling for gas migration

Currently, the most common industry approaches to predicting gas migration are purely qualitative risk analyses through special numbers[1,43,44]. These approaches can offer, at most, a quick look method to discriminate between risky cement sheath designs from those that are less risky for gas migration. However, to efficiently evaluate the risk of gas migration, it is necessary to have a model that allows computing at each time the properties of casing/cement/formation and the state of temperature, pressure, stress, pore pressure (when applicable) within each component of the wellbore. Listed below is a small sample of work that the industry has done over the years.

Sutton and Ravi[22] measured permeability of cement during hydration using a U-tube filled with cement and water on top. The authors suggested that cement permeability decreases when the SGS increases, leading to a reduction of transmissibility of hydrostatic pressure from the top to bottom of the cement column.

Appleby and Wilson[45] used the poro-elastic theory to calculate the decrease of hydrostatic pressure during hydration. Their formulation can be used when cement is a porous solid, but cannot be used to explain loss of hydrostatic pressure of cement columns in earlier periods.

Sabins et al.[10] argued that the reduction of hydrostatic pressure is equal to the friction between cement and formation/casing, which originates from SGS development. They gave an expression of the hydrostatic-pressure loss accounting for the reduction of cement volume and the compressibility of cement. They also presented the first model that aims at predicting gas invasion during the cement's transition period. Some of the model hypotheses were:

- Fluid loss from the slurry does not contribute to loss of hydrostatic pressure when restriction to pressure transmission has not started to develop.
- Measurable SGS can result in pressure restriction along the cement column, provided that the cement volume decreases.
- A decrease in the water volume within the cement results from hydration and fluid loss and causes a decrease in cement pressure.
- The resulting pressure against the formation face is a function of transmitted hydrostatic pressure as long as the pressure restriction resulting from SGS development has not become greater than the pressure loss resulting from the volume reduction.
- When pressure restriction resulting from SGS development becomes greater than the pressure loss resulting from the volume reduction, the cement is completely isolated from the hydrostatic pressure, and pressure loss is a function of water volume reductions and slurry compressibility.
- If calculated cement pressure falls below the gas zone pressure before the end of the transition time, annular gas flow is predicted.

Chenevert and Jin[46] model is an extension of the previous model in three manners: 1) It is written through differential equations; 2) It accounts for the increase of cement density as a result of bulk shrinkage; and 3) It replaces the SGS concept by the more sophisticated elastic-plastic rheology concept.

Daccord and Baret[47] assumed that: 1) SGS evolves according to an exponential law; 2) Shrinkage evolves according to a Poisson's law; 3) Fluid losses can be evaluated from Darcy's law in the presence of both mud cake and cement cake; and 4) Cement density increases as a result of its compressibility.

Prohaska et al.[48,49] assumed that, during transition time, when hydrostatic pressure falls to gas pressure value, gas starts invading the cement column but the gas bubbles need to have sufficiently large volumes in order to detach from the formation walls and follow the Archimedes' effect They also introduced the concept of the critical distance within the cement sheath where gas inflow can occur, a point of view that seems to be also shared by other authors[36,50].

The model of Prohaska et al. allows accounting for the effect of filter cake and for the influence of slurry shearing, temperature, and pressure on the development of SGS. Higher shear rates result in SGS retardation and an increase in temperature or in pressure accelerates SGS development. These results, which imply that SGS develops faster in the lower part of a uniform cement column, are in agreement with the concepts of maturity and equivalent age. However, the model does not go that far and does not present a global formulation to take shear rate, temperature and pressure into account.

Sabins and Wiggins[51] presented a model that postulates that cement slurry behaves like a porous body when it is in transitional phase, that Darcy equation is valid, that there is an infinite source of water on the top of cement column, and that no water inflow occurs from the formation toward the cement sheath. If volume losses produce a pressure decrease less than that allowed by the SGS, the actual pressure drop is computed using Darcy equation. On the other hand, if a volume change occurs that produces a larger pressure decrease than that per-

mitted by SGS development, a downward movement of the column occurs.

Zhou and Wojtanowicz[52] argued that the reduction of hydrostatic pressure is influenced not only by the compressibility of cement but also by that of the formation and casing. They combined the effect of the reduction of volume due to shrinkage and fluid loss with the compressibility of the system due to variation of stresses and temperature in order to model the hydrostatic pressure loss.

Nishikawa et al.[53] stated that, at early time, the volume reduction is essentially attributed to the fluid loss because the chemical shrinkage is not sufficiently high and that the friction force between cement and casing or formation is not important on pressure loss, which is in contradiction with most hypotheses of previous works. They also accounted for an observation made that fluid-loss rate is constant and small (equivalent to API drilling mud fluid loss of approximately 1 cc/30 min) as a function of time over relatively long time intervals. This result contradicts the conventional theory of constant pressure cake filtration but makes sense if the pressure decreases during the filtration.

Synthesis of the literature review on gas migration

- Gas migration can occur anytime during the life of the well, in particular during the well cementing job and shortly after the cement is in place.
- The evolution of the static gel strength (SGS) is one of the main factors of the decrease of hydrostatic pressure in the cement column.
- Once the hydrostatic pressure becomes lower than the pore pressure in the formation, fluid can migrate into cement column if a leakage pathway is available.
- There exist more than one mechanism that can explain the decrease in slurry pressure and only using the SGS parameter to predict gas migration does not allow creating a holistic method that will work in all cases[54].
- Due to many factors there is not one unique potential leakage pathway.
- Most, if not all models developed in the past to predict gas migration only focus on the liquid stage of the cement sheath, and did not fully simulate cement hydration towards a porous solid.

As a consequence, evaluating the risk of gas migration requires a new model that simulates the cement sheath throughout the entire cement column, starting from after bumping the plug, and looking at all previously described mechanisms. To do this requires a model that is able to take into account:

- The various physical stages of cement life (liquid and porous solid).
- The various formations encountered along the well depth.
- The changes of cement properties, temperature, pore pressures and stresses versus depth and time.
- The various mechanisms that can lead to pressure decrease to below reservoir pressure.
- The various mechanisms that can lead to the connectivity (leak path) from one gas reservoir to another reservoir or to the surface.

New model for stress modeling in the cement sheath at early age

General concepts

The new model is based on the simulation of cement hydration. After cement is mixed, its hydration degree and properties evolve with time as a result of various chemical reactions. This evolution depends on temperature, stresses, and water exchanges between the cement and the formation. A hydration model that allows simulating this hydration process has been developed and its validation has been presented in another paper[55]. It allows computing various cement properties as a function of the degree of hydration or as a function of time, such as porosity, shrinkage, elastic properties (Young's modulus, Poisson's ratio), plastic behavior, failure properties (cohesion, friction angle) and heat transfer properties (conductivity, specific heat).

Cement hydration is modeled according to an Arrhenius thermo-activated process. The chemical affinity depends not only on cement composition, water-to-cement ratio, Blaine fineness of cement powder, but also on the diffusion of water through hydrate layers and the actual hydration degree. The effects of temperature and pressure are taken into account.

During hydration, hydrates are formed around anhydrate grains to form larger grains. At the beginning, the slurry behaves as a suspension of grains in water. At a given porosity, these grains start to contact with adjacent ones. This porosity is called the percolation porosity and is similar to the "critical porosity" of granular materials. The related degree of hydration is called the percolation hydration degree or percolation threshold. Its value depends on cement composition, water-to-cement ratio, and the type of additives. Inert additives are simulated through the theory of inclusions, while reactive additives modify the kinetics of cement hydration.

The model assumes that cement mechanical properties, such as drained bulk and shear moduli, bulk modulus of solid phase, UCS, TS, drained thermal expansion coefficient and friction angle, are functions of the hydration degree, water-to-cement ratio, and temperature, according to non linear laws. Use is made of poro-mechanics and homogenization theories to evaluate these nonlinear functions.

Cement behavior after percolation is simulated according to thermo-chemo-poro-elasto-plasticity. Therefore, there is no need to guess the state of stress in the cement during hydration, because the state of stress is directly computed.

Swelling/shrinkage of cement comes from hydration heat (thermal expansion), water consumption by chemical reactions (leading to a decrease in pore pressure), cement grain volume increase, and water exchange with formation.

Hypotheses

The model detailed in the following parts has been simplified, to keep it easily understandable. The hypotheses are the following:

- The cement sheath has the shape of a cylinder, with outer and inner radii of r_i and r_{i+1}.

- The wellbore is vertical. Removing this hypothesis is very simple.
- Real well geometry is taken into account;
- The evolution of all cement parameters versus the hydration degree is known.
- Cement thermo-poro-elastic law, when cement is a porous solid, writes[56]:

$$\underline{\underline{\delta\sigma}} = \left(K_d - \frac{2G}{3}\right)\cdot tr\,\underline{\underline{\delta\varepsilon}}\cdot\underline{\underline{I}} + 2G\cdot\underline{\underline{\delta\varepsilon}} + b\cdot\delta p_p\cdot\underline{\underline{I}} + 3K_d\cdot\left(s_d\cdot\delta\xi + \alpha_d\cdot\delta T\right)\cdot\underline{\underline{I}}$$

$$\delta p_p = M\cdot\left(b\cdot tr\,\underline{\underline{\delta\varepsilon}} + \frac{\delta m}{\rho_l}\right) + 3\frac{K_u\cdot\alpha_u - K_d\cdot\alpha_d}{b}\cdot\delta T - 3\frac{K_u\cdot s_u + K_d\cdot s_d}{b}\cdot\delta\xi$$

This shows that there is an analogy between the thermo-elastic, poro-elastic, and chemo-elastic behaviors. Knowing Lamé's formulas for thick cylinders in thermo-elasticity[57], allows evaluating the equivalent formulas for poro-elasticity, and chemo-elasticity.

- The cement pore pressure remains above vaporization pressure, meaning that the cement remains saturated by water.
- Temperature, cement hydration, and pore pressure do not depend on radius of the cement sheath.
- Cement hydration is modeled according to an Arrhenius thermo-activated law.
- Fluid loss is taken into account by using some of the models published in the literature[1,46,48,53], even if it is not presented here below, due to the desire to simplify the presentation of the model
- The boundary conditions at the cement sheath interfaces (the superscript (i) denotes cement outer interface, while the superscript (i+1) denotes cement inner interface) are of constant rigidity:

In the absence of micro-annulus at outer interface:

$$dp_M^{(i)} = -k_i\cdot\left[\frac{du_r^{(i)}}{r_i} + \left(1+\nu_i\right)\cdot\alpha_i\cdot dT^{(i)}\right]$$

In the presence micro-annulus at outer interface:

$$dp_M^{(i)} = dp_p$$

In the absence of micro-annulus at inner interface:

$$dp_M^{(i+1)} = k_{i+1}\cdot\left[\frac{du_r^{(i+1)}}{r_{i+1}} + \left(1+\nu_{i+1}\right)\cdot\alpha_{i+1}\cdot dT^{(i+1)}\right]$$

In the presence of micro-annulus at inner interface:

$$dp_M^{(i+1)} = dp_p$$

Some of the hypotheses can easily be removed, but were set to simplify the presentation of the model.

Cement sheath hydration before percolation without sliding

The problem is considered as the superposition of two sub-problems:

- The sub-problem of hydration under constant volume. The cement slurry being a fluid, the equations used to compute stresses and displacements take the following form:

$$d\sigma_{zz} = d\sigma_{\theta\theta} = d\sigma_{rr} = 3K_f\cdot\left(-s\cdot d\xi + \alpha\cdot dT\right)$$

$$d\sigma_{rz} = d\sigma_{r\theta} = d\sigma_{\theta z} = 0 \qquad du_z = du_\theta = du_r = 0$$

- The sub-problem of the application of a vertical displacement on cement slurry at a given hydration degree under isothermal condition.

The state of stress is isotropic in a fluid, therefore, the boundary conditions can be written:

$$du_r^{(i)} = -r_i\cdot\left[\frac{d\sigma_{zz}}{k_i} + \left(1+\nu_i\right)\cdot\alpha_i\cdot dT^{(i)}\right]$$

$$du_r^{(i+1)} = r_{i+1}\cdot\left[\frac{d\sigma_{zz}}{k_{i+1}} - \left(1+\nu_{i+1}\right)\cdot\alpha_{i+1}\cdot dT^{(i+1)}\right]$$

The variation of the volume of fluid writes:

$$dV = \left(u_z - du_z\right)\cdot\left(A + dA\right) - u_z\cdot A$$

With:

$$dA = -2\pi\cdot\left(r_i - du_r^{(i)} - r_{i+1} - du_r^{(i+1)}\right) \qquad A = \pi\cdot\left(r_i^2 - r_{i+1}^2\right)$$

This gives

$$\frac{dA}{A} = -2\cdot\frac{r_i}{r_i^2 - r_{i+1}^2}\cdot du_r^{(i)} + 2\cdot\frac{r_{i+1}}{r_i^2 - r_{i+1}^2}\cdot du_r^{(i+1)}$$

Therefore:

$$\frac{dA}{A} = \frac{2}{r_i^2 - r_{i+1}^2}\cdot\begin{vmatrix} -r_{i+1}^2\cdot\left(1+\nu_{i+1}\right)\cdot\alpha_{i+1}\cdot dT^{(i+1)} \\ +\left(\frac{r_i^2}{k_i} + \frac{r_{i+1}^2}{k_{i+1}}\right)\cdot d\sigma_{zz} \\ +r_i^2\cdot\left(1+\nu_i\right)\cdot\alpha_i\cdot dT^{(i)} \end{vmatrix}$$

The volumetric strain can be written:

$$d\varepsilon = -\frac{dV}{V} = \frac{du_z}{z} - \frac{dA}{A} = d\varepsilon_{zz} - \frac{dA}{A}$$

Which gives:

$$d\varepsilon = -\frac{dV}{V} = \frac{du_z}{z} - \frac{2}{r_i^2 - r_{i+1}^2}\cdot\begin{vmatrix} -r_{i+1}^2\cdot\left(1+\nu_{i+1}\right)\cdot\alpha_{i+1}\cdot dT^{(i+1)} \\ +\left(\frac{r_i^2}{k_i} + \frac{r_{i+1}^2}{k_{i+1}}\right)\cdot d\sigma_{zz} \\ +r_i^2\cdot\left(1+\nu_i\right)\cdot\alpha_i\cdot dT^{(i)} \end{vmatrix}$$

The variation of the vertical stress is defined as:

$$d\sigma_{zz} = -K_f\cdot\frac{dV}{V}$$

This gives:

$$d\sigma_{zz} = \Xi\cdot\begin{vmatrix} \left(1-\chi^2\right)\cdot d\varepsilon_{zz} \\ +2\cdot\chi^2\cdot\left(1+\nu_{i+1}\right)\cdot\alpha_{i+1}\cdot dT^{(i+1)} \\ -2\cdot\left(1+\nu_i\right)\cdot\alpha_i\cdot dT^{(i)} \end{vmatrix}$$

Where:

$$\Xi = \frac{\kappa_i\kappa_{i+1}\cdot K_f}{\left(1-\chi^2\right)\cdot\kappa_i\kappa_{i+1} + 2\cdot\left(\kappa_{i+1} + \kappa_i\cdot\chi^2\right)}$$

And

$$\kappa_i = \frac{k_i}{K_f} \qquad \kappa_{i+1} = \frac{k_{i+1}}{K_f}$$

Therefore, the stress and displacement fields are summarized as:

$$d\sigma_{zz} = d\sigma_{\theta\theta} = d\sigma_{rr} = \Xi\cdot\begin{vmatrix} \left(1-\chi^2\right)\cdot d\varepsilon_{zz} \\ +2\cdot\chi^2\cdot\left(1+\nu_{i+1}\right)\cdot\alpha_{i+1}\cdot dT^{(i+1)} \\ -2\cdot\left(1+\nu_i\right)\cdot\alpha_i\cdot dT^{(i)} \end{vmatrix}$$

$$d\sigma_{rz} = d\sigma_{r\theta} = d\sigma_{\theta z} = 0$$

$$\frac{du_r^{(i)}}{r_i} = -\frac{\Xi}{\kappa_i \kappa_{i+1} \cdot K_f} \cdot \begin{vmatrix} \left(1-\chi^2\right)\cdot\kappa_{i+1}\cdot d\varepsilon_{zz} \\ +2\cdot\chi^2\cdot\kappa_{i+1}\cdot\left(1+\nu_{i+1}\right)\cdot\alpha_{i+1}\cdot dT^{(i+1)} \\ +\kappa_i\cdot\left[\kappa_{i+1}\cdot\left(1-\chi^2\right)+2\cdot\chi^2\right]\cdot\left(1+\nu_i\right)\cdot\alpha_i\cdot dT^{(i)} \end{vmatrix}$$

$$\frac{du_r^{(i+1)}}{r_{i+1}} = \frac{\Xi}{\kappa_i \kappa_{i+1} \cdot K_f} \cdot \begin{vmatrix} \left(1-\chi^2\right)\cdot\kappa_i\cdot d\varepsilon_{zz} \\ -\left[\left(1-\chi^2\right)\cdot\kappa_i+2\right]\cdot\kappa_{i+1}\cdot\left(1+\nu_{i+1}\right)\cdot\alpha_{i+1}\cdot dT^{(i+1)} \\ -2\cdot\kappa_i\cdot\left(1+\nu_i\right)\cdot\alpha_i\cdot dT^{(i)} \end{vmatrix}$$

Cement sheath hydration after percolation without sliding

Cement hydration formulas, under generalized plane strain condition, are obtained by the superposition of four sub-problems worked out under undrained conditions:

- The sub-problem of non-isotherm cement hydration under plane strain condition, with no changes of pore pressure besides the changes that happen due to cement hydration and with no applied pressures at boundary. It can easily be solved based on Lamé's formulas for thermo-elasticity and chemo-elasticity.
- The sub-problem of changes of pore pressure under plane strain condition, for example due to the diffusion of pore pressure through the cement, and with no applied pressures at boundary. It can easily be solved based on Lamé's formulas in poro-elasticity.
- The sub-problem of applied pressures at cement-sheath boundary associated with an additional constant axial stress to obtain a plane strain solution. It can easily be solved based on Lamé's formulas in plane strain condition.
- The sub-problem of applied axial stress, which is used to break the plane strain condition when the cement sheath slides axially.

The displacement and stress fields write:

$$\overrightarrow{du} = \underline{\underline{C}}_{u1}\cdot\overrightarrow{d\Sigma_1} + \overrightarrow{C_{du2}}\cdot dp_a + \overrightarrow{du_0}$$

$$\overrightarrow{d\sigma} = \underline{\underline{C}}_{d\sigma 1}\cdot\overrightarrow{d\Sigma_1} + \overrightarrow{C_{d\sigma 2}}\cdot dp_a + \overrightarrow{d\sigma_0}$$

$$dp_p = \underline{\underline{C}}_{dp1}\cdot\overrightarrow{d\Sigma_1} + \frac{h\cdot B}{3}\cdot dp_a + dp_0$$

Where:

$${}^t\overrightarrow{d\sigma} = \begin{bmatrix} d\sigma_{rr} & d\sigma_{\theta\theta} & d\sigma_{zz} & d\sigma_{r\theta} & d\sigma_{\theta z} & d\sigma_{zr} \end{bmatrix}$$

$${}^t\overrightarrow{du} = \begin{bmatrix} du_r & du_\theta & du_z \end{bmatrix} \qquad {}^t\overrightarrow{d\Sigma_1} = \begin{bmatrix} dp^{(i)} & dp^{(i+1)} \end{bmatrix}$$

$${}^t\underline{\underline{C}}_{u1} = \frac{1}{2G}\cdot\frac{1}{1-\chi^2}\cdot\frac{r_{i+1}}{x}\times\begin{Bmatrix} \left(1-2\nu\right)+x^2 & 0 & 0 \\ -\left(1-2\nu\right)\cdot\chi^2 - x^2 & 0 & 0 \end{Bmatrix}$$

$${}^t\overrightarrow{C_{du2}} = \frac{1}{E}\cdot\begin{Bmatrix} -\nu\cdot\frac{r_{i+1}}{x} & 0 & z \end{Bmatrix}$$

$${}^t\overrightarrow{du_0} = \frac{r_{i+1}}{x}\cdot\begin{bmatrix} -\frac{\chi^2}{1-\chi^2}\cdot\left(1-2\nu+x^2\right)\cdot dJ_\chi - x^2\cdot dJ_x & 0 & 0 \end{bmatrix}$$

$$\underline{\underline{C}}_{d\sigma 1} = \frac{1}{1-\chi^2}\cdot\begin{Bmatrix} 1-x^2 & -\chi^2+x^2 \\ 1+x^2 & -\chi^2-x^2 \\ 2\nu & -2\nu\cdot\chi^2 \\ 0 & 0 \\ 0 & 0 \\ 0 & 0 \end{Bmatrix} \qquad \overrightarrow{C_{d\sigma 2}} = \begin{Bmatrix} 0 \\ 0 \\ 1 \\ 0 \\ 0 \\ 0 \end{Bmatrix}$$

$$\overrightarrow{d\sigma_0} = 2G\cdot\begin{bmatrix} x^2\cdot dJ_x - \frac{1-x^2}{1-\chi^2}\cdot\chi^2 dJ_\chi \\ dJ - \frac{1+x^2}{1-\chi^2}\cdot\chi^2\cdot dJ_\chi - x^2\cdot dJ_x \\ dJ - 2\nu\cdot\frac{\chi^2}{1-\chi^2}\cdot dJ_\chi \\ 0 \\ 0 \\ 0 \end{bmatrix}$$

$$\underline{\underline{C}}_{dp1} = h\cdot\frac{2\cdot B}{3}\cdot\left(1+\nu\right)\cdot\frac{1}{1-\chi^2}\cdot\begin{bmatrix} 1 & -\chi^2 \end{bmatrix}$$

$$dp_0 = dK' - 2\frac{h\cdot B\cdot E}{3}\cdot\frac{\chi^2}{1-\chi^2}\cdot dJ_\chi$$

It is assumed that fluid loss is negligible, even if it can easily be included if required.

Combining boundary conditions with the cement hydration formulas allows writing:

$$dp_M^{(i)} = 2G\cdot\begin{vmatrix} +\frac{\left(k_{i+1}+2G\right)\cdot k_i\cdot d\pi_{10}}{\left(1-2\nu\right)\cdot k_i k_{i+1}+2G\cdot k_i\cdot\pi_{11}+2G\cdot k_{i+1}\cdot\pi_{12}+4G^2} \\ -\frac{k_i\left(k_{i+1}\cdot\pi_{12}+2G\right)\cdot\left(1+\nu_i\right)\cdot\alpha_i\cdot dT^{(i)}}{\left(1-2\nu\right)\cdot k_i k_{i+1}+2G\cdot k_i\cdot\pi_{11}+2G\cdot k_{i+1}\cdot\pi_{12}+4G^2} \\ +\frac{2\left(1-\nu\right)\cdot k_i k_{i+1}\cdot\pi_2\cdot\left(1+\nu_{i+1}\right)\cdot\alpha_{i+1}\cdot dT^{(i+1)}}{\left(1-2\nu\right)\cdot k_i k_{i+1}+2G\cdot k_i\cdot\pi_{11}+2G\cdot k_{i+1}\cdot\pi_{12}+4G^2} \end{vmatrix}$$

$$dp_M^{(i+1)} = 2G\cdot\begin{vmatrix} +\frac{\left(k_i-2G\right)\cdot k_{i+1}\cdot d\pi_{10}}{\left(1-2\nu\right)\cdot k_i k_{i+1}+2G\cdot k_i\cdot\pi_{11}+2G\cdot k_{i+1}\cdot\pi_{12}+4G^2} \\ -\frac{2\left(1-\nu\right)\cdot k_i k_{i+1}\cdot\pi_1\cdot\left(1+\nu_i\right)\cdot\alpha_i\cdot dT^{(i)}}{\left(1-2\nu\right)\cdot k_i k_{i+1}+2G\cdot k_i\cdot\pi_{11}+2G\cdot k_{i+1}\cdot\pi_{12}+4G^2} \\ +\frac{\left(k_i\cdot\pi_{11}+2G\right)\cdot k_{i+1}\cdot\left(1+\nu_{i+1}\right)\cdot\alpha_{i+1}\cdot dT^{(i+1)}}{\left(1-2\nu\right)\cdot k_i k_{i+1}+2G\cdot k_i\cdot\pi_{11}+2G\cdot k_{i+1}\cdot\pi_{12}+4G^2} \end{vmatrix}$$

As a result, the displacement and stress fields write:

$$\frac{x}{r_{i+1}}\cdot du_r = \frac{1}{1-\chi^2}\cdot\begin{vmatrix} +\left(1-\nu\right)\cdot\begin{bmatrix} -\left(1-\chi^2\right)+\left(1-2\nu\right)\cdot\pi_{13} \\ +\left(1-2\nu\right)\cdot\chi^2\cdot\pi_{15}+x^2\cdot\pi_{14} \end{bmatrix}\cdot C_{10}\cdot d\xi \\ +\left(1-\nu\right)\cdot\begin{bmatrix} -\left(1-\chi^2\right)+\left(1-2\nu\right)\cdot\pi_{13} \\ +\left(1-2\nu_{hyd}\right)\cdot\chi^2\cdot\pi_{15}+x^2\cdot\pi_{14} \end{bmatrix}\cdot C_9\cdot dT \\ -\left[\left(1-2\nu\right)\cdot\pi_{13}+x^2\cdot\pi_{16}\right]\cdot\left(1+\nu_i\right)\cdot\alpha_i\cdot dT \\ -\left[\left(1-2\nu\right)\cdot\chi^2\cdot\pi_{15}+x^2\cdot\pi_{17}\right]\cdot\left(1+\nu_{i+1}\right)\cdot\alpha_{i+1}\cdot dT \\ +\left(1-\nu\right)\cdot\begin{bmatrix} -\left(1-\chi^2\right)+\left(1-2\nu\right)\cdot\pi_{13} \\ +\left(1-2\nu\right)\cdot\chi^2\cdot\pi_{15}+x^2\cdot\pi_{14} \end{bmatrix}\cdot C_{11}\cdot dp_{pores} \\ +\begin{bmatrix} -\left(1-\chi^2\right)+\left(1-2\nu\right)\cdot\pi_{13} \\ +\left(1-2\nu\right)\cdot\chi^2\cdot\pi_{15}+x^2\cdot\pi_{14} \end{bmatrix}\cdot\frac{\nu}{E}\cdot dp_a \end{vmatrix}$$

$$\frac{1}{z}\cdot du_z = \frac{1}{E}\cdot dp_a$$

$$d\sigma_{rr} = \frac{2G}{1-\chi^2}\cdot\begin{vmatrix} +\left(1-\nu\right)\cdot\left(\pi_{13}+\chi^2\cdot\pi_{15}-x^2\cdot\pi_{14}\right)\cdot C_{10}\cdot d\xi \\ +\left(1-\nu\right)\cdot\left(\pi_{13}+\chi^2\cdot\pi_{15}-x^2\cdot\pi_{14}\right)\cdot C_{9}\cdot dT \\ -\left(\pi_{13}-x^2\cdot\pi_{16}\right)\cdot\left(1+\nu_i\right)\cdot\alpha_i\cdot dT \\ -\left(\chi^2\cdot\pi_{15}-x^2\cdot\pi_{17}\right)\cdot\left(1+\nu_{i+1}\right)\cdot\alpha_{i+1}\cdot dT \\ +\left(1-\nu\right)\cdot\left(\pi_{13}+\chi^2\cdot\pi_{15}-x^2\cdot\pi_{14}\right)\cdot C_{11}\cdot dp_{pores} \\ +\left(\pi_{13}+\chi^2\cdot\pi_{15}-x^2\cdot\pi_{14}\right)\cdot\frac{\nu}{E}\cdot dp_a \end{vmatrix}$$

$$d\sigma_{\theta\theta} = \frac{2G}{1-\chi^2}\cdot\begin{vmatrix} +\left(1-\nu\right)\cdot\left(\pi_{13}+\chi^2\cdot\pi_{15}+x^2\cdot\pi_{14}\right)\cdot C_{10}\cdot d\xi \\ +\left(1-\nu\right)\cdot\left(\pi_{13}+\chi^2\cdot\pi_{15}+x^2\cdot\pi_{14}\right)\cdot C_{9}\cdot dT \\ -\left(\pi_{13}+x^2\cdot\pi_{16}\right)\cdot\left(1+\nu_i\right)\cdot\alpha_i\cdot dT \\ -\left(\chi^2\cdot\pi_{15}+x^2\cdot\pi_{17}\right)\cdot\left(1+\nu_{i+1}\right)\cdot\alpha_{i+1}\cdot dT \\ +\left(1-\nu\right)\cdot\left(\pi_{13}+\chi^2\cdot\pi_{15}+x^2\cdot\pi_{14}\right)\cdot C_{11}\cdot dp_{pores} \\ +\left(\pi_{13}+\chi^2\cdot\pi_{15}+x^2\cdot\pi_{14}\right)\cdot\frac{\nu}{E}\cdot dp_a \end{vmatrix}$$

$$d\sigma_{zz} = \frac{2G}{1-\chi^2}\cdot\begin{vmatrix} +\left(1-\nu\right)\cdot\left[2\nu\cdot\left(\pi_{13}+\chi^2\cdot\pi_{15}\right)+\left(1-\chi^2\right)\right]\cdot C_{10}\cdot d\xi \\ +\left(1-\nu\right)\cdot\left[2\nu\cdot\left(\pi_{13}+\chi^2\cdot\pi_{15}\right)+\left(1-\chi^2\right)\right]\cdot C_{9}\cdot dT \\ -2\nu\cdot\pi_{13}\cdot\left(1+\nu_i\right)\cdot\alpha_i\cdot dT \\ -2\nu\cdot\chi^2\cdot\pi_{15}\cdot\left(1+\nu_{i+1}\right)\cdot\alpha_{i+1}\cdot dT \\ +\left(1-\nu\right)\cdot\left[2\nu\cdot\left(\pi_{13}+\chi^2\cdot\pi_{15}\right)+\left(1-\chi^2\right)\right]\cdot C_{11}\cdot dp_{pores} \\ +\left[\left(\pi_{13}+\chi^2\cdot\pi_{15}\right)\cdot\frac{2\nu^2}{E}+\frac{1-\chi^2}{2G}\right]\cdot dp_a \end{vmatrix}$$

$$dp_p = \frac{1}{1-\chi^2}\cdot\begin{vmatrix} +\left[2\left(1-\nu\right)\cdot\left(\pi_{13}+\chi^2\cdot\pi_{15}\right)\cdot C_{10}\cdot C_{15}+\left(1-\chi^2\right)\cdot C_{18}\right]\cdot d\xi \\ +\left[2\left(1-\nu\right)\cdot\left(\pi_{13}+\chi^2\cdot\pi_{15}\right)\cdot C_{9}\cdot C_{15}+\left(1-\chi^2\right)\cdot C_{17}\right]\cdot dT \\ -2C_{15}\cdot\pi_{13}\cdot\left(1+\nu_i\right)\cdot\alpha_i\cdot dT \\ -2C_{15}\cdot\chi^2\cdot\pi_{15}\cdot\left(1+\nu_{i+1}\right)\cdot\alpha_{i+1}\cdot dT \\ +\left[2\left(1-\nu\right)\cdot\left(\pi_{13}+\chi^2\cdot\pi_{15}\right)\cdot C_{11}\cdot C_{15}+\left(1-\chi^2\right)\cdot C_{20}\right]\cdot dp_{pores} \\ +\left[2C_{15}\cdot\left(\pi_{13}+\chi^2\cdot\pi_{15}\right)\cdot\frac{\nu}{E}+\left(1-\chi^2\right)\cdot C_{16}\right]\cdot dp_a \end{vmatrix}$$

Solving for sliding

The axial strain within the porous solid cement sheath generates antiplane shear stresses, which can be computed based on the following equations[57]:

$$du_r = du_\theta = 0$$

$$\frac{x}{r_{i+1}}\cdot du_z = -\frac{1}{G}\cdot\frac{1}{1-\chi^2}\cdot\left[\left(1+x^2\right)\cdot d\sigma_{zr}^{(i+1)}-\left(\chi^2+x^2\right)\cdot d\sigma_{zr}^{(i)}\right]$$

$$d\sigma_{zr} = \frac{1}{1-\chi^2}\cdot\left[\left(1-x^2\right)\cdot d\sigma_{zr}^{(i+1)}-\left(\chi^2-x^2\right)\cdot d\sigma_{zr}^{(i)}\right]$$

$$d\sigma_{\theta z} = dp_p = 0$$

The solution of cement hydration and sliding after percolation contains three unknowns: Two shear stresses at cement sheath interfaces, $\sigma_{rz}^{(i+1)}$, $\sigma_{rz}^{(i)}$ and the applied stress p_a for the porous solid case, or the applied axial strain ε_{zz} for the liquid case. These variables are computed by:

- Splitting the cement sheath into n axial elements with a grid with nodes j=1 to n+1, and writing the equilibrium of each element of the cement-sheath column.

$$\sigma_{zz}^{(j+1)}-\sigma_{zz}^{(j)}+\rho_{ce}\cdot g\cdot\left(z_{j+1}-z_j\right)=\frac{2\cdot\left(z_{j+1}-z_j\right)}{\left(r_i^2-r_{i+1}^2\right)}\cdot\left(r_{i+1}\cdot\sigma_{zr}^{(i+1)(j)}+r_i\cdot\sigma_{zr}^{(i)(j)}\right)$$

- Writing the equilibrium of each element of the cement-sheath column during the increment of time dt.

$$2\frac{r_{i+1}\cdot d\sigma_{zr}^{(i+1)(j-1)}+r_j\cdot d\sigma_{zr}^{(i)(j-1)}}{r_i^2-r_{i+1}^2}=-\frac{d\sigma_{zz}^{(j)}-d\sigma_{zz}^{(j-1)}}{z_j-z_{j-1}}$$

- Taking into account a Mohr-Coulomb friction criterion at the interfaces that tells when sliding occurs.

$$\text{No sliding}\leftrightarrow\begin{vmatrix}\tau_{\max}^{(i+1,j)}<SGS^{(j)}+\left(\sigma_{rr}^{(i+1,j)}-p_p^{(i+1,j)}\right)\cdot\tan\varphi^{(j)}\\ \tau_{\max}^{(i,j)}<SGS^{(j)}+\left(\sigma_{rr}^{(i,j)}-p_p^{(i,j)}\right)\cdot\tan\varphi^{(j)}\end{vmatrix}$$

$$\text{Sliding}\leftrightarrow\begin{vmatrix}\tau_{\max}^{(i+1,j)}=SGS^{(j)}+\left(\sigma_{rr}^{(i+1,j)}-p_p^{(i+1,j)}\right)\cdot\tan\varphi^{(j)}\\ \tau_{\max}^{(i,j)}=SGS^{(j)}+\left(\sigma_{rr}^{(i,j)}-p_p^{(i,j)}\right)\cdot\tan\varphi^{(j)}\end{vmatrix}$$

The friction angle is null when the cement is a fluid.

- Adapting the values of the applied stress p_a or the applied axial strain ε_{zz} such that, 1) if no sliding occurs within a given element during an increment of time dt, they are null; but 2) if sliding occurs, their value is chosen for Mohr-Coulomb to be exactly checked at the cement sheath interfaces.

Gas migration mechanisms

When the various stresses, pore pressure, and properties of the cement are known as a function of time, any gas migration initiation criterion can be analyzed to evaluate if one of them is checked, and when this occurs:

- Gas flow through the cement matrix occurs when the gas pressure is larger than the cement pore pressure.
- Gas bubbling takes place based on criteria such as described by Govier and Aziz[34], Dubash and Friggard[35], and Pinto et al.[36].
- Micro-annulus at the cement/casing interface is based on a tensile strength criterion.
- Micro-annulus at the cement/formation interface is based on a tensile strength criterion.
- Shear failure of cement is based on Mohr-Coulomb criterion.
- Tensile failure of cement is based on a tensile strength criterion.

However, gas migration initiation is not a critical criterion because it does not tell if a loss of integrity will occur, and if so, where will the gas flow, and at which flow rate.

Therefore more advanced works should be engaged to quantify fluid flows, such as the work presented by Lecampion et al.[58] on micro-annulus propagation.

Example of the use of the model

A case study of a vertical well is presented; the well architecture is shown in Figure 2. The well has a 28" conductor casing set and cemented at 600 m. A 22" casing is set and cemented at 1,500 m. The system used to cement the 28" by 22" annulus has a density of 1.72 SG and a 10-hr total thickening time. The 22" casing is cemented to the sea floor using a 1.5 SG mud to displace the cement from the casing. A washout of 36" is formed under the 28" casing shoe at the beginning of the drilling of the 26" openhole.

A 12 MPa gas formation is encountered at 900 m. Excluding the gas formation all other formations encountered during drilling are mudstones. The 1.72 SG cement system is the target of the gas migration investigation. The mechanical and thermal properties of the cement and formation used as inputs are presented in Table 1.

Table 1. Set cement and formation properties

Parameter	Unit	Cement	Formation
Young's modulus	GPa	7.0	5.0
Poisson's ratio	-	0.25	0.20
Friction angle	°	15	-
Thermal conductivity	W/m/K	0.9	2.0
Specific heat	J/kg/K	2000	1200
Drained volumetric thermal expansion coefficients	1/°C	8.0×10^{-5}	-

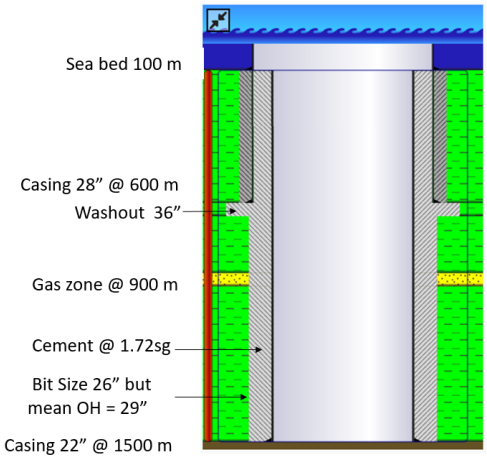

Figure 2. Well architecture

The results of the simulations are shown in Figures 3 - 10.

Figure 3 shows the evolution of temperature at different well depths. Initially the cement sheath is heated by the formation. At the 4-hrs mark, cement hydration begins, which leads to a rapid increase of temperature. After 15 hrs, the temperature decreases with time along the cement sheath proving that heat diffused to the formation is higher than the heat obtained due to cement chemical reactions. The cement sheath experiences a lower rate of temperature increase in the cased hole section (depths lower than 600 m) as compared to in the open hole section (depth higher than 600m). The temperature is highest at 600 m due to the 36" washout under the 28" casing shoe because the temperature increase is a function of the thickness of the cement sheath.

Figure 4 compares the evolution of hydration degree at 100 m, 600 m and 1500 m. We can notice that the hydration degree at 600 m is impacted by the presence of the washout while at 100 m, the hydration degree increases more slowly. This is in agreement with the evolution of the temperature shown in Figure 3.

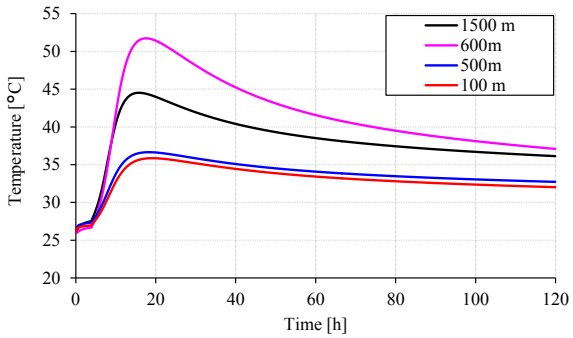

Figure 3. Temperature of cement vs. time after cement placement

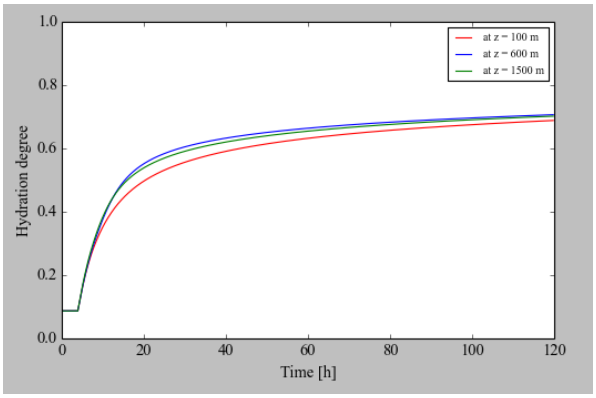

Figure 4. Hydration degree vs. time after cement placement

Figures 5-7 show that the cement pore pressure, radial and vertical stresses increase due to the increase in temperature. After percolation, cement chemical expansion and thermal expansion lead to a pore pressure increase. The increase rate is highest at 600 m due to the highest increase rate of temperature. Then temperature decrease and chemical shrinkage lead to a reduction in cement pore pressure, radial and vertical stresses.

Figure 5 indicates that:

- Cement desaturation occurs around the 40-hr mark at the top of the cement. It occurs faster at shallow well depths than at deeper depths.
- At the gas formation depth of 900 m, the pore pressure in the cement before the 50-hrs mark is greater than the gas formation pore pressure.
- After the 50-hrs mark, the pore pressure of the formation is greater that the pore pressure in the cement sheath, which can lead to gas migration into the cement column.

Figure 6 indicates that the radial stress decreases much faster at the cement/casing interface than at the cement/formation interface. This can be explained by the fact that a micro-annulus has opened at the cement/casing interface, which induces a very fast decrease in radial stress at this interface because it is then equal to cement pore pressure.

Figure 7 shows that the vertical stress at the top of cement remains constant and equal to 1.5 MPa, which is equal to the mud pressure above the cement column.

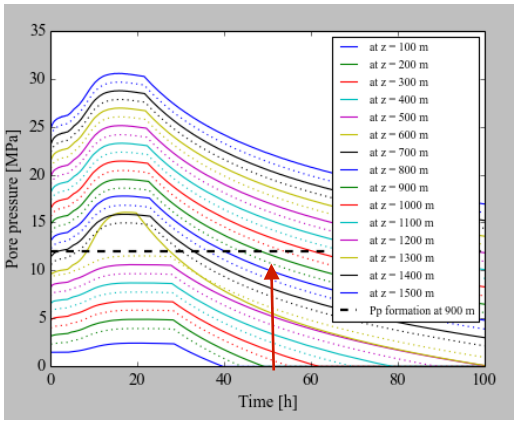

Figure 5. Pore pressure vs. time after cement placement (solid: inner interface; dashed: outer interface)

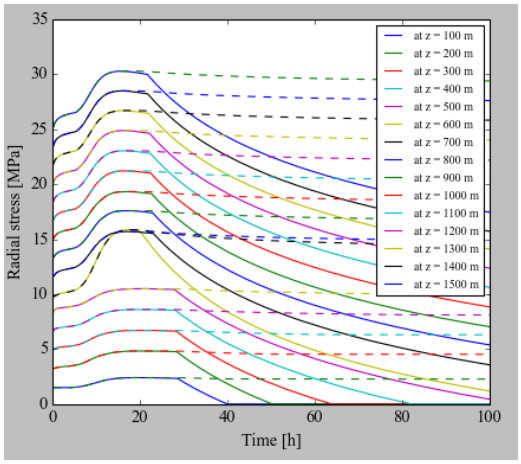

Figure 6. Radial stress vs. time after cement placement (solid: inner interface; dashed: outer interface)

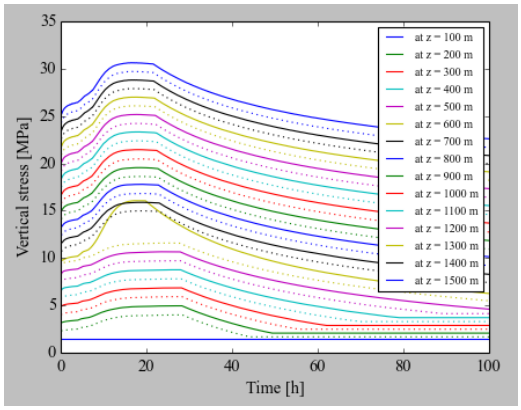

Figure 7. Vertical stress vs. time after cement placement

Figure 8 presents the evolution of a micro-annulus width at casing-cement sheath interface (inner interface) versus time at various wellbore depths. The micro-annulus width is highest at the 36" washout at 600 m. The figure also points out that the micro-annulus width is lower above the 28" casing due to a smaller thickness of the cement sheath.

Figure 9 presents the computed micro-annulus width at 100 hrs. A micro-annulus only occurs at the casing-cement interface (inner interface); its aperture varies between 100 µm to 300 µm, which is sufficient to create a pathway for gas migration. Figure 9 also indicates that a micro-annulus between the cement and formation or between the cement and 28" casing (outer interface) does not occur. Due to micro-annulus at casing-cement interface, gas migration may occur after the casing is perforated and the gas formation is brought onto production.

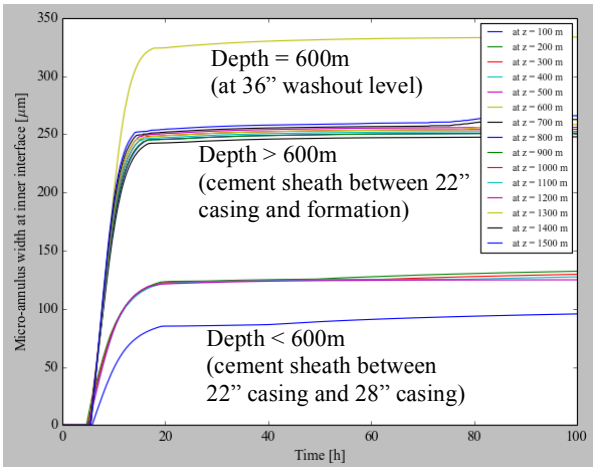

Figure 8. Evolution of micro-annulus width at inner interface vs. time at different depths

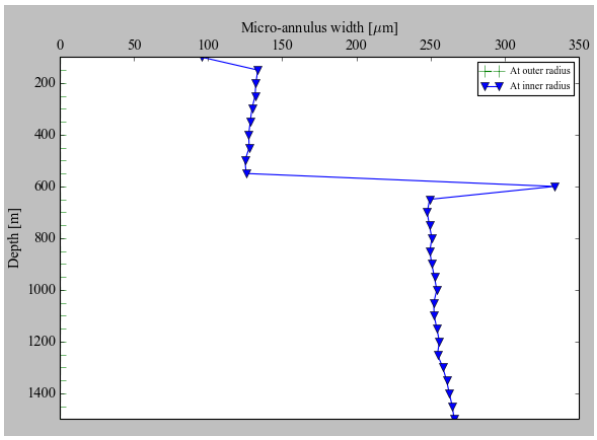

Figure 9. Evolution of micro-annulus width at 100 h vs. depth

Figure 10 indicates evolution of the axial displacement of the cement sheath versus time. At the 4-hr mark, the temperature increases rapidly, which leads to an upward movement of cement at depths lower than 600 m. Due to the presence of the washout under the 28" casing shoe, the axial displacement

is blocked at 600 m. After 15-hrs, the temperature decreases, and the shrinkage of cement leads to a downward displacement. However, the shear stress between the cement and the formation is sufficient to block the axial displacement and to decrease the pore pressure and stresses in the cement.

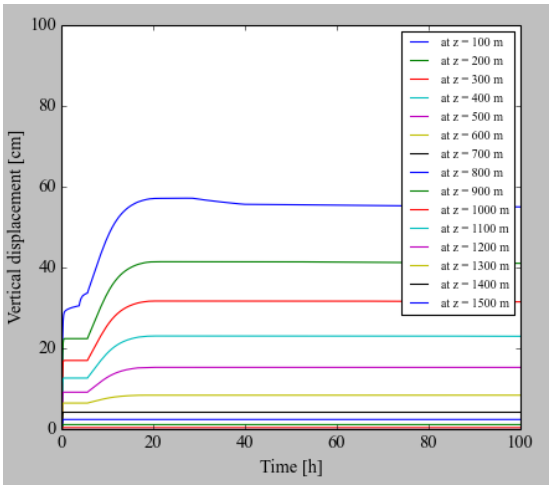

Figure 10. Evolution of vertical displacement vs. time

As a conclusion, a micro-annulus opens at the casing/cement interface 5 hrs after the cement placement, but cement pore pressure is larger than formation gas pressure. Therefore there is no gas migration. After 50 hrs, the cement pore pressure becomes less than the formation pore pressure allowing gas migration. However, unless the cement sheath fails by disking, the gas should first diffuse through the cement-sheath thickness before reaching the micro-annulus and move towards the surface. This means that, even if gas migration will occur, its magnitude may not be very large.

In order to investigate the effect of the washout under 28" casing shoe, the simulation is repeated while not considering this washout. Therefore, Figure 11 and Figure 12 show the evolution of micro-annulus width at 100 h versus depth and the evolution of the vertical displacement versus time for the case without the 36" washout under the 28" casing shoe.

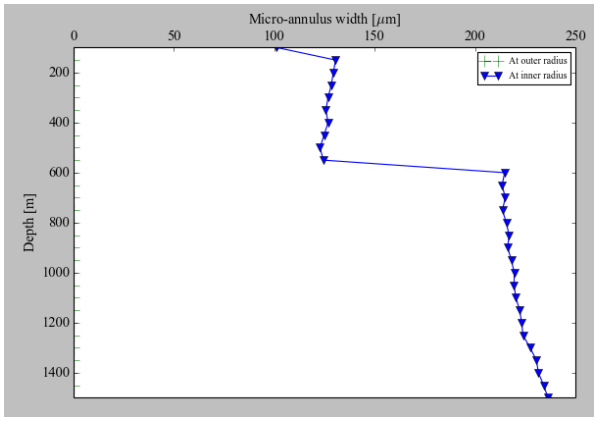

Figure 11. Evolution of micro-annulus width at 100 h vs. depth with no washout

Figure 11 indicates that the micro-annulus width at low depths does not depend on the existence of the washout below the 28" casing shoe but that, below the shoe, the washout tends to result in a wider micro-annulus. For example, at 600 m, the micro-annulus width is 210 μm when there is no washout, against a value of 340 μm in the presence of the washout.

Furthermore, Figure 12 points out that the vertical displacement under the 28" casing shoe is no more blocked, resulting in a higher upward movement of the top of cement.

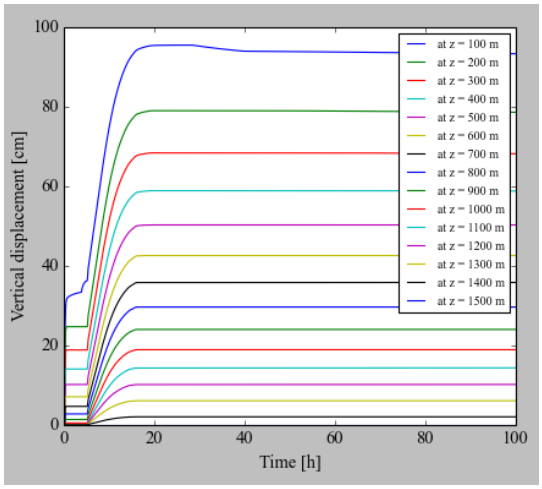

Figure 12. Evolution of vertical displacement vs. time with no washout

Conclusions

A model has been presented, which allows computing, at any depth and any time, especially at early age, the cement properties, state of stress, and the pore pressure. This model considers the complete well as composite and interdependent structure and not only the materials it is made of (steel casing, cement and surrounding formation).

Therefore, it is possible to check any gas migration criterion: Darcy flow, bubbling, micro-annulus, shear damage, and tensile damage.

The example of the use of the model has shown that:

- It is important to correctly take into account the real geometry of wellbore. For example, the presence of washouts modifies the vertical displacements that take place within the cement sheath during cement hydration and, as a consequence, the micro-annulus width.
- Cement heat of hydration induces changes of stresses and pore pressure which, if not taken into account, could make the model non predictive.
- The cement desaturation can occur and, if it occurs, it happens sooner at shallow depths.
- The opening of a micro-annulus is not always associated with gas migration. For example when the cement pore pressure remains larger than the formation pressure, the underbalanced condition of gas migration is not checked, meaning that gas migration is not possible.
- Gas flow may occur when the cement pore pressure

becomes less than the formation pressure (underbalanced condition), but the flow rate may not only be governed by the micro-annulus aperture, but also by the capacity of the gas to diffuse through the thickness of the cement sheath: Gas migration may use a combination of leakage paths for gas to reach another reservoir or the surface.

Nomenclature

α	= *Cement linear thermal expansion coefficient*
α_i	= *Outer interface linear thermal expansion coefficient*
α_{i+1}	= *Inner interface linear thermal expansion coefficient*
α_m	=*Cement isochoric fluid mass influx coefficient*
ε	= *Strain*
λ	= *Cement Lamé's coefficient*
ν	= *Cement Poisson's ratio*
ν_i	= *Outer interface Poisson's ratio*
ν_{i+1}	= *Inner interface Poisson's ratio*
ξ	= *Hydration degree*
π_i	= *Constant*
σ	= *Stress*
χ	= *Radius ratio*
A	= *Section of the cement sheath*
B	= *Cement Skempton's coefficient*
CHA	= *Cement hydration analyzer*
C_i	= *Constant*
$CSGS$	= *Critical static gel strength*
E	= *Cement Young's modulus*
G	= *Cement shear modulus*
I_y	= *Constant*
J	= *Constant*
J_y	= *Constant*
K	= *Cement Bulk modulus*
K'	= *Constant*
M	= *Cement Biot's modulus*
OD	= *Outer diameter*
SCV	= *Surface casing-vents*
SGS	= *Static gel strength*
T	= *Temperature*
V	= *Volume*
b	= *Cement Biot's coefficient*
h	= *Constant*
k_i	= *Outer interface rigidity*
k_{i+1}	= *Inner interface rigidity*
p_a	= *Applied axial pressure*
p_{pores}	= *Applied pore pressure*
s	= *Cement linear shrinkage coefficient*
s_m	= *Cement isochoric fluid mass influx coefficient for cement hydration*
u	= *Displacement*
x	= *Radius ratio*

References

1. Stiles, D.: "Annular Formation Fluid Migration", in Well Cementing, Erik B. Nelson and Dominique Guillot, Eds, 2nd edition, Chapter 9, 289-318.
2. Stone, W.H. and Christian, W.W.: "The Inability of Unset Cement to Control Formation Pressure" SPE 4783, SPE Symposium on Formation Damage Control, New Orleans, Louisiana, USA, February 7-8, 1974.
3. Garcia, J.A. and Clark, C.R.: "An Investigation of Annular Gas Flow Following Cementing Operations", SPE 5701, SPE Symposium on Formation Damage Control, Houston, Texas, USA, January 29–30, 1976.
4. Cooke, C.E., Kluck, M.P., and Medrano, R.: "Field Measurements of Annular Pressure and Temperature During Primary Cementing", Journal of Petroleum technology, v. 35, No.8, (August 1983) 1429-1438.
5. Al Buraik, K., Al Abdulqader, K., and Bsaibes, R.: "Prevention of Shallow Gas Migration Through Cement", IADC/SPE 47775, IADC/SPE Asia Pacific Drilling Conference, Jakarta, Indonesia, September 7-9, 1998.
6. Bour, D.L. and Wilkinson, J.G.: "Combating Gas Migration in the Michigan Basin", SPE Drilling Engineering, v. 7, No.1, (March 1992) 65-71.
7. Carter, L.G. and Slagle, K.: "A Study of Completion Practices to Minimize Gas Communication", Journal of Petroleum Technology, v. 24, No.9, (September 1972) 1170-1174.
8. Carter, L.G., Cook, C., Jr., and Snelson, L.: "Cementing Research in Directional Gas Well Completion", SPE 4313, SPE Annual European Meeting, London, UK, April 2-3, 1973.
9. Webster, W.W. and Eikerts, J.V.: "Flow After Cementing - A Field and Laboratory Study", SPE 8259, SPE Annual Fall Technical Conference and Exhibition, Las Vegas, Nevada, USA September 23-26, 1979.
10. Sabins, F.L., Tinsley, J.M., and Sutton, D.L.: "Transition Time of Cement Slurries Between the Fluid and Set States", SPE Journal, 22, No.6, (June 1982) 875–882.
11. Bannister, C.E., Shuster, G.E., Wooldridge, L.A., Jones, M.J., and Birch, A.G.: "Critical Design Parameters to Prevent Invasion During Cementing Operations", SPE 11982, SPE Annual Technical Conference and Exhibition, San Francisco, California, USA, October 5-8, 1983.
12. Beirute, R.M. and Cheung, P.R.: "A Method for Selection of Cement Recipes to Control Fluid Invasion After Cementing", SPE Production Engineering, v. 5, No.11, (November 1990) 433-440.
13. Levine, D.C., Thomas, E.W., Bezner, H.P., and Tolle, G.C.: "Annular Gas Flow After Cementing: A Look at Practical Solutions", SPE 8255, SPE Annual Fall Technical Conference, Las Vegas, Nevada, USA, September 23-26, 1979.
14. Tinsley, J.M., Miller, E.C., Sabins, F.L., and Sutton, D.L.: "Study of Factors Causing Annular Gas Flow Following Primary Cementing", Journal of Petroleum Technology, v. 32, No.8, (August 1980) 1427–1437.
15. Cheung, P.R. and Beirute, R.M.: "Gas Flow in Cements", Journal of Petroleum Technology, v. 37, No.6 (June 1985) 1041–1048.
16. Parcevaux, P.A. and Sault, P.H.: "Cement Shrinkage and Elasticity: A New Approach for a Good Zonal Isolation", SPE 13176, SPE Annual Technical Conference and Exhibition, Houston, Texas, USA, September 16-19, 1984.
17. Stewart, R.B. and Schouten, F.C.: "Gas Invasion and Migration in Cemented Annuli: Causes and Cures", SPE Drilling Engineering, v. 3, No.1, (March 1988) 77–82.
18. Sykes, R.L. and Logan, J.L.: "New Technology in Gas Migration Control", SPE 16653, SPE Annual Technical Conference and Exhibition, Dallas, Texas, USA, September 27-30, 1987.

19 Dean, G.D. and Brennen, M.A.: "A Unique Laboratory Gas Flow Model Reveals Insight to Predict Gas Migration in Cement", SPE 24049, SPE Western Regional Meeting, Bakersfield, California, USA, March 30-April 1, 1992.

20 Watters, L.T. and Sabins, F.L.: "Field Evaluation of Method to Control Gas Flow Following Cementing", SPE 9287, SPE Annual Fall Technical Conference and Exhibition, Dallas, Texas, USA, September 21-24, 1980.

21 Seidel, F.A. and Greene, T.G.: "Use of Expanding Cement Improves Bonding and Aids in Eliminating Annular Gas Migration in Hobbs Grayburg-San Andres Wells", SPE 14434, SPE Annual Technical Conference and Exhibition, Las Vegas, Nevada, USA, September 22-25, 1985.

22 Sutton, D.L. and Ravi. K.M.: "New Method for Determining Dowhole Properties That Affect Gas Migration and Annular Sealing", SPE 19520, SPE Annual Technical Conference and Exhibition, San Antonio, Texas, USA, October 8-11, 1989.

23 Rae, Phil, Wilkins, D., and Free, D.: "A New Approach to the Prediction of Gas Flow After Cementing", SPE/IADC 18622, SPE/IADC Drilling Conference, New Orleans, Louisiana, USA, February 28-March 3, 1989.

24 Tahmourpour, F., Hashki, K., and Hassan, H.: "Different Methods to Avoid Annular Pressure Buildup by Appropriate Engineered Sealant and Applying Best Practices (Cementing and Drilling) ", SPE Drilling & Completion, v. 25, No.2, (June 2010) 248-252.

25 Bonett A. and Pafitis D.: "Getting to the Root of Gas Migration", Oilfield Review, v. 8; No.1, (Spring 1996) 36-49.

26 Wojtanowicz, A.K., Manowski, W., and Nishikawa, S.: "Gas Flow in Wells After Cementing", Technical report, Louisiana State University, Baton Rouge, Louisiana, USA (September 2000) 58.

27 Drecq, P. and Parcevaux, P.A.: "A Single Technique Solves Gas Migration Problems Across a Wide Range of Conditions", SPE 17629, SPE International Meeting on Petroleum Engineering, Tianjin, China, November, 1-4, 1988.

28 Christian, W.W., Chatterji, J., and Ostroot, G.W.: "Gas Leakage in Primary Cementing – A Field Study and Laboratory Investigation", Journal of Petroleum Technology, v. 28, No.11, (November 1976), 1361-1369.

29 Garcia, J.A. and Clark, C.R.: "An Investigation of Annular Gas Flow Following Cementing Operations", SPE 5701, SPE Symposium on Formation Damage Control, Houston, Texas, USA, January 29–30, 1976.

30 Cook, C. and Cunningham, W.C.: "Filtrate Control—A Key in Successful Cementing Practices", Journal of Petroleum Technology, v. 29, No.8, (August 1977) 951–956.

31 Baret, J.F.: "Why Cement Fluid Loss Additives Are Necessary", SPE 17630, SPE International Meeting on Petroleum Engineering, Tianjin, China, November, 1-4 1988.

32 Carter, L.G. and Evans, G.W.: "A Study of Cement-Pipe Bonding", Journal of Petroleum Technology, v. 16, No.2, (February 1964) 157-160.

33 Dean, G.D. and Brennen, M.A.: "A Unique Laboratory Gas Flow Model Reveals Insight to Predict Gas Migration in Cement", SPE 24049, SPE Western Regional Meeting, Bakersfield, California, USA, March 30-April 1, 1992.

34 Govier, G.W. and Aziz, K.: "The Flow of Complex Mixtures in Pipes", Van Nostrand (1972) 820.

35 Dubash, N. and Frigaard, I.A.: "Conditions for Static Bubbles in Viscoplastic Fluids", Physics of Fluids, v. 16, No.12, (2004) 4319-4330.

36 Pinto, G.H.V.P, Martins, A.L., Rocha, J.M.S., and Martinelli, A.E.: "New Methodology for Gas Migration Prediction Before Oilwell Cementing", Brazilian Journal of Petroleum and Gas, v. 6, No.2, (2012) 67-78.

37 Bois, A.-P., Garnier, A., Rodot, F., Saint-Marc, J., and Aimard, N.: "How to Prevent Loss of Zonal Isolation Through a Comprehensive Analysis of Microannulus Formation", SPE Drilling & Completion v. 26, No.1, (March 2011) 13-31.

38 Bois, A.-P., Garnier, A., Galdiolo, G., and Laudet, J.-B.: "Use of a Mechanistic Model to Forecast Cement-Sheath Integrity", SPE Drilling & Completion, v. 27, No.2, (June 2012) 304-314.

39 Shipley S.E. and Mitchell B.J.: "The Effect of Hole Inclination on Gas Migration", SPE 20432, SPE Annual Technical Conference and Exhibition, New Orleans, Louisiana, USA, September 23-26, 1990.

40 Ladva, H.K.J., Craster, B., Jones, T.G.J, Goldsmith, G., and Scott, D.: "The Cement-To-Formation Interface in Zonal Isolation", SPE Drilling & Completion, v. 20, No.3 (September 2005) 186-197.

41 Martins, A.L., Campos, G., Silva, M.G.P., Miranda, C.R., and Teixeira, K.C.: "Tools for Predicting and Avoiding Gas Migration After Casing Cementing in Brazilian Fields", SPE 39008, SPE Latin American and Caribbean Petroleum Engineering Conference and Exhibition, Rio de Janeiro, Brazil, August 30-September 3, 1997.

42 Degouy, D.G. and Large, P.R.: "An Innovative Cell to Control the Gas-Tightness of Cement Slurries", SPE 28473, SPE Annual Technical Conference and Exhibition, New Orleans, Louisiana, USA, September 25-28, 1994.

43 Sutton, D.L. and Faul, R.: "Annular Gas Flow Theory and Prevention Methods described," Oil & Gas Journal (December 10, 1984) 82, 50, 84–86.

44 Rae, Ph., Wilkins, D., and Free, D.: "A New Approach to the Prediction of Gas Flow After Cementing", SPE/IADC 18622, SPE/IADC Drilling Conference, New Orleans, Louisiana, USA, February 28-March 3, 1989.

45 Appleby, S. and Wilson, A.: "Permeability and Suction in Setting Cement", Chemical Engineering Science, v. 51, No.2, (1996) 251-267.

46 Chenevert, M.E. and Jin, L.: "Model for Predicting Wellbore Pressures in Cement Columns", SPE 19521, SPE Annual Technical Conference and Exhibition, San Antonio, Texas, USA, October 8-11, 1989.

47 Daccord, G. and Baret, J.F.: "How Fluid Loss Influences Primary Cementing: Literature Review and Methodology," SPE Drilling & Completion, v. 9, No.2, (June 1994) 133-138.

48 Prohaska, M., Ogbe, D.O., and Economides, M.J.: "Determining Wellbore Pressure in Cement Slurry Columns", SPE 26070, SPE Western Regional Meeting, Anchorage, Alaska, USA (May 26-28,1993).

49 Prohaska, M, Fruhwirth, R., and Economides, M.J.: "Modeling Early-Time Gas Migration Through Cement Slurries", SPE Drilling and Completion, v. 10, No.3, (September 1995) 178-185.

50 Xu, R.: "Analysis of Diagnostic Testing of Sustained Casing Pressure in Wells", PhD thesis, Louisiana State University and Agriculture and Mechanical College (2002) 142.

51 Sabins, F.L. and Wiggins, M.L. "Parametric Study of Gas Entry into Cemented Wellbores", SPE Drilling & Completion, v. 12, No. 3, (September 1997) 180-187.

52 Zhou, D. and Wojtanowicz, A.K.: "New Model of Pressure Reduction to Annulus During Primary Cementing", IADC/SPE 59137, IADC/SPE Drilling Conference, New Orleans, Louisiana, USA, February 23–25, 2000.

53 Nishikawa, S. and Wojtanowicz, A.K.: "Transient Pressure Unloading – A Model of Hydrostatic Pressure Loss in Wells After Cement Placement", SPE 77754, SPE Annual Technical Conference and Exhibition, San Antonio, Texas, USA, September 29-October 2, 2002.
54 Li, Z., Vandenbossche, J.M., Iannacchione, T., Brigham, J.C., and Kutchko, B.G.: "Theory-Based Review of Limitations with Static Gel Strength in Cement/Matrix Characterization", SPE Drilling & Completion, v. 31, No.2, (May 2016) 145-158.
55 Thérond, E., Bois, A.-P, Whaley, K., and Murillo, R.: "Large Scale Testing & Modeling for Cement Zonal Isolation of Water Injection Wells", SPE 181428, SPE Annual Technical Conference and Exhibition, Dubai, UAE (September 26-28, 2016).
56 Garnier, A., Saint-Marc, J., Laudet, J.-B., Rodot, F., Urbanczyk, C., and Bois, A.-P.: "Well Integrity", in Carbon Capture and Storage - The Lacq pilot - Project and injection period 2006-2013 (2015) 68.
57 Timoshenko, S. and Goodier, J.N.: "Theory of elasticity", McGraw-Hill, 1951, 506.
58 Lecampion, B., Bunger, A., Kear, J., and Quesada, D.: "Interface Debonding Driven by Fluid Injection in a Cased and Cemented Wellbore: Modeling and Experiments", International Journal of Greenhouse Gas Control, v. 18, (October 2013) 208–223.

Appendix. Constants formulas

Various constant are used in the appendix. They are defined here below, where the index d or u to denote drained or undrained regime is omitted.

$$\alpha_m = \frac{\alpha_u \cdot K_u - \alpha_d \cdot K_d}{b \cdot M} \qquad s_m = \frac{s_u \cdot K_u + s_d \cdot K_d}{b \cdot M}$$

$$h = \begin{cases} 0 \text{ if drained} \\ 1 \text{ if undrained} \end{cases} \qquad C_9 = \frac{1+\nu}{1-\nu} \cdot \alpha$$

$$C_{10} = \frac{(1-2h)\cdot(1+\nu)}{1-\nu} \cdot s \qquad C_{11} = \frac{h \cdot (1+\nu) \cdot b}{3(1-\nu)\cdot K}$$

$$C_{12} = h \cdot M \cdot \left(3\alpha_m - \frac{1+\nu}{1-\nu} \cdot b \cdot \alpha\right) \qquad C_{13} = -h \cdot M \cdot \left(3s_m - \frac{1+\nu}{1-\nu} \cdot b \cdot s\right)$$

$$C_{15} = \frac{h \cdot B \cdot E}{3} \qquad C_{16} = \frac{h \cdot B}{3}$$

$$C_{17} = h \cdot M \cdot \left[3\alpha_m - 2(1+\nu) \cdot b \cdot \alpha\right] \qquad C_{18} = -h \cdot M \cdot \left[3s_m - 2(1+\nu) \cdot b \cdot s\right]$$

$$C_{19} = h \cdot \left(1 - \frac{1+\nu}{1-\nu} \cdot \frac{Bb}{3}\right) \qquad C_{20} = h \cdot \left[1 - 2(1+\nu) \cdot \frac{Bb}{3}\right]$$

$$x = \frac{r_{i+1}}{r} \qquad \chi = \frac{r_{i+1}}{r_i} \qquad I_y(dZ) = \left(\frac{1-y^2}{2y^2}\right) \cdot dZ$$

$$dJ_y = \left(\frac{1-y^2}{2y^2}\right) \cdot \left[C_9 \cdot dT + C_{10} \cdot d\xi + C_{11} \cdot dp_{pores}\right]$$

$$dJ = C_9 \cdot dT + C_{10} \cdot d\xi + C_{11} = \frac{h \cdot (1+\nu) \cdot b}{3(1-\nu)\cdot K} \cdot dp_{pores}$$

$$dK' = C_{12} \cdot dT + C_{13} \cdot d\xi + C_{19} \cdot dp_{pores}$$

$$\pi_1 = \frac{1}{1-\chi^2} \qquad \pi_2 = \frac{\chi^2}{1-\chi^2}$$

$$d\pi_{10} = \frac{\nu}{E} \cdot dp_a + (1-\nu) \cdot \left[C_9 \cdot dT + C_{10} \cdot d\xi + C_{11} \cdot dp_{pores}\right]$$

$$\pi_{11} = (1-2\nu) \cdot \pi_1 + \pi_2 \qquad \pi_{12} = \pi_1 + (1-2\nu) \cdot \pi_2$$

$$\pi_{13} = \frac{(2G + k_{i+1}) \cdot k_i}{(1-2\nu) \cdot k_i k_{i+1} + 2G \cdot k_i \cdot \pi_{11} + 2G \cdot k_{i+1} \cdot \pi_{12} + 4G^2}$$

$$\pi_{14} = \frac{2G \cdot (k_i + k_{i+1})}{(1-2\nu) \cdot k_i k_{i+1} + 2G \cdot k_i \cdot \pi_{11} + 2G \cdot k_{i+1} \cdot \pi_{12} + 4G^2}$$

$$\pi_{15} = \frac{(2G - k_i) \cdot k_{i+1}}{(1-2\nu) \cdot k_i k_{i+1} + 2G \cdot k_i \cdot \pi_{11} + 2G \cdot k_{i+1} \cdot \pi_{12} + 4G^2}$$

$$\pi_{16} = \frac{\left[2G - (1-2\nu) \cdot k_{i+1}\right] \cdot k_i}{(1-2\nu) \cdot k_i k_{i+1} + 2G \cdot k_i \cdot \pi_{11} + 2G \cdot k_{i+1} \cdot \pi_{12} + 4G^2}$$

$$\pi_{17} = \frac{\left[2G + (1-2\nu) \cdot k_i\right] \cdot k_{i+1}}{(1-2\nu) \cdot k_i k_{i+1} + 2G \cdot k_i \cdot \pi_{11} + 2G \cdot k_{i+1} \cdot \pi_{12} + 4G^2}$$